Electronic Supplementary Material (ESI) for CrystEngComm

Nickel(II)thiocyanato Coordination Compounds: Synthetic Aspects, Polymorphism, Thermal Reactivity and Magnetic Properties

Jan Boeckmann, Nils Evers and Christian Näther*

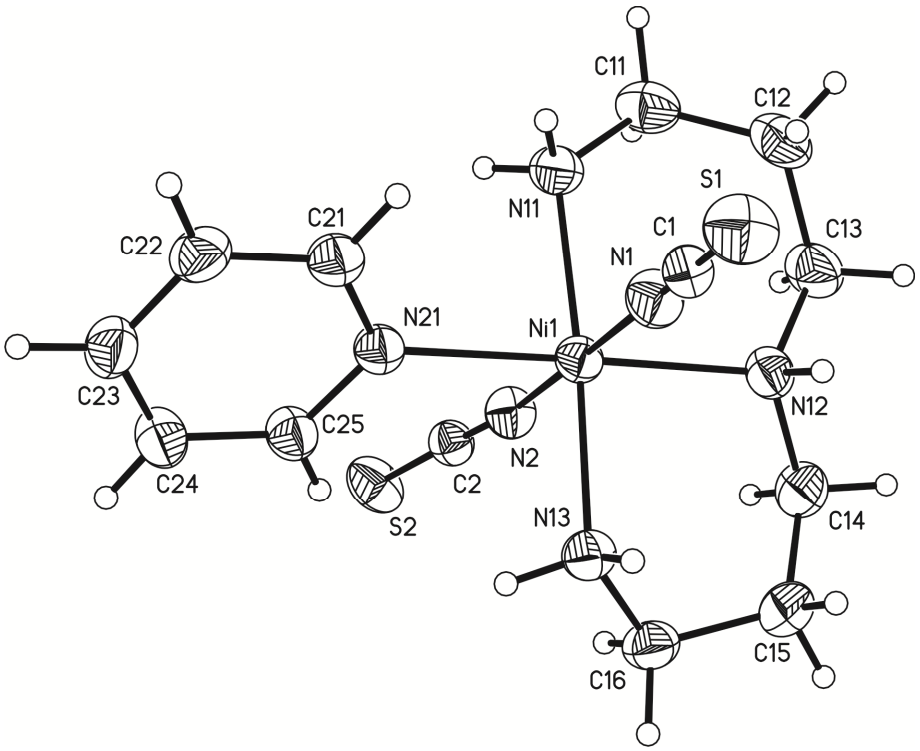

Figure S1. Crystal structure of compound **1II** with labeling and displacement ellipsoids drawn at the 50 % probability level.

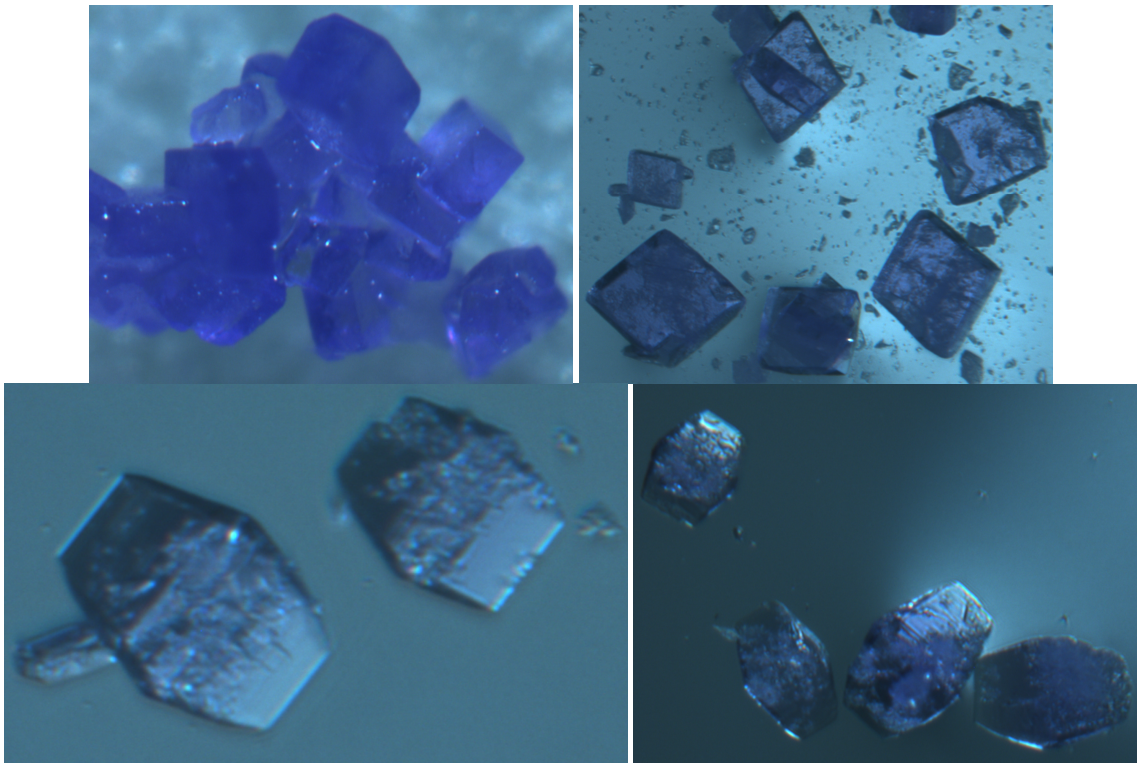

Figure S2. Pictures of the single-crystals of the polymorphic modifications **1I** (top) and **1II** (bottom).

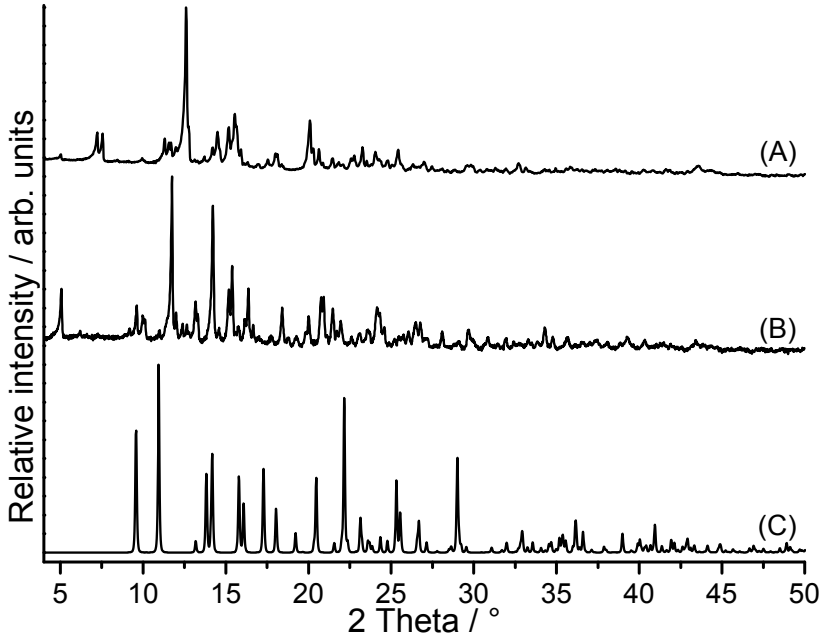

Figure S3. Experimental XRPD patterns of the residues obtained in the first TG step in the thermal decomposition reaction of compounds **1I** (A) and **4** (B), together with XRPD pattern calculated from single-crystal data for compound $[Ni(SCN)_2(dpt)]_2$ (**5**) (C).

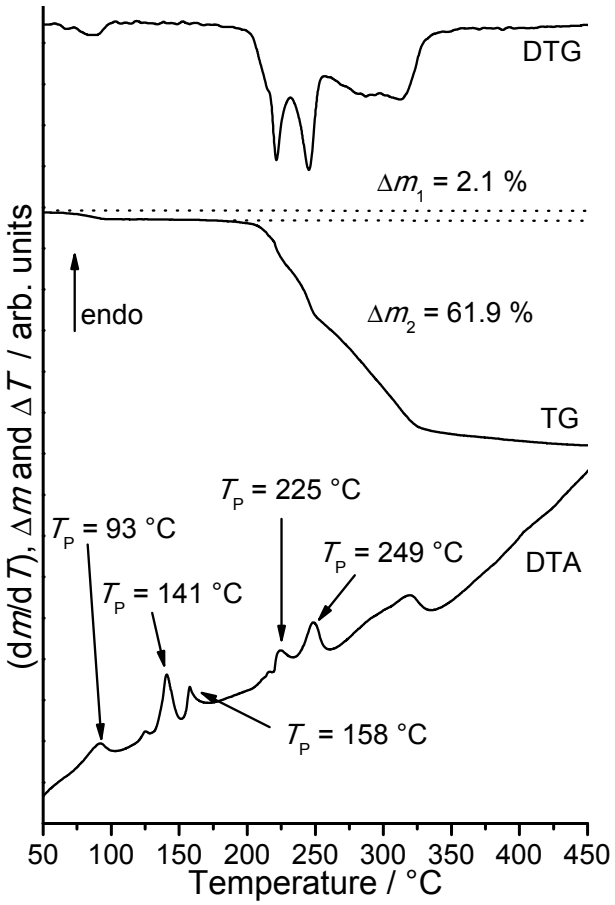

Figure S4. DTG, TG and DTA curves of compound **3**. Heating rate = 4 °C min^{-1}; given are the mass changes [%] and the peak temperatures T_P [°C].

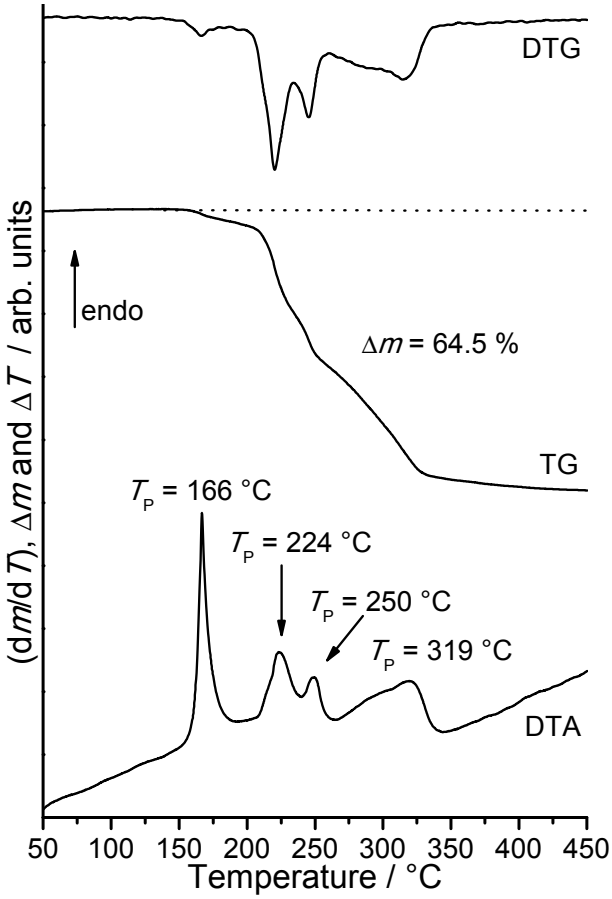

Figure S5. DTG, TG and DTA curves of compound **2**. Heating rate = 4 °C min^{-1}; given are the mass changes [%] and the peak temperatures T_P [°C].

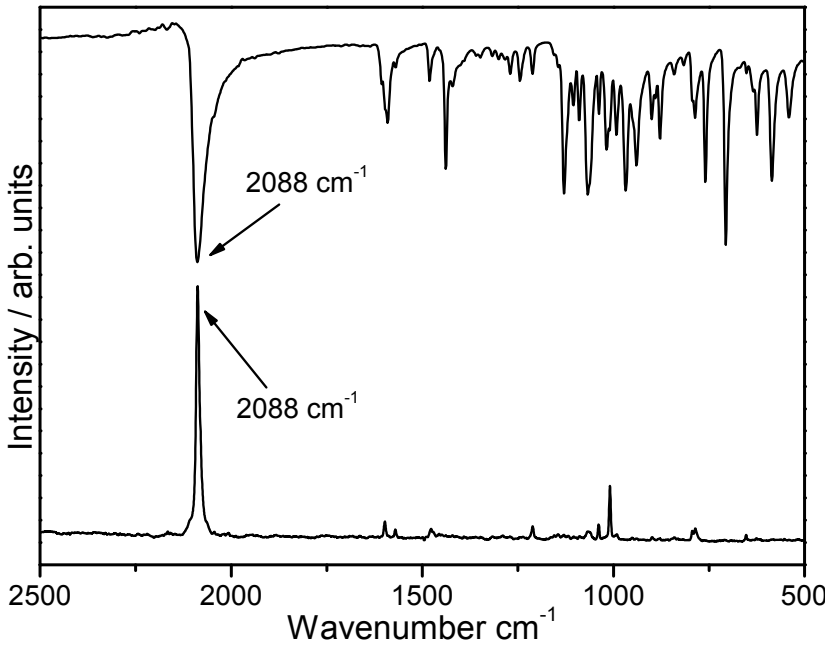

Figure S6. IR (top) and Raman (bottom) spectra for compound **1I**.

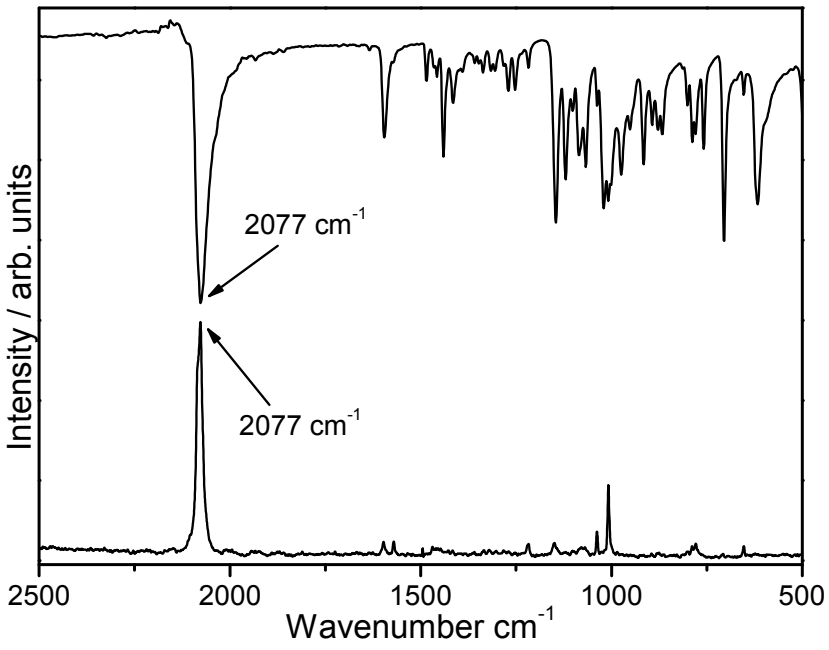

Figure S7. IR (top) and Raman (bottom) spectra for compound **1II**.

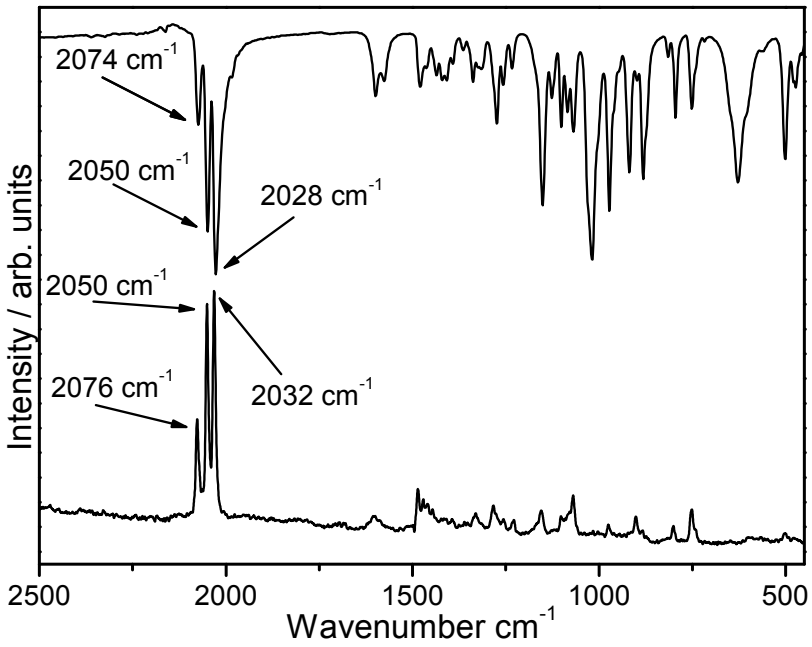

Figure S8. IR (top) and Raman (bottom) spectra for compound **2**.

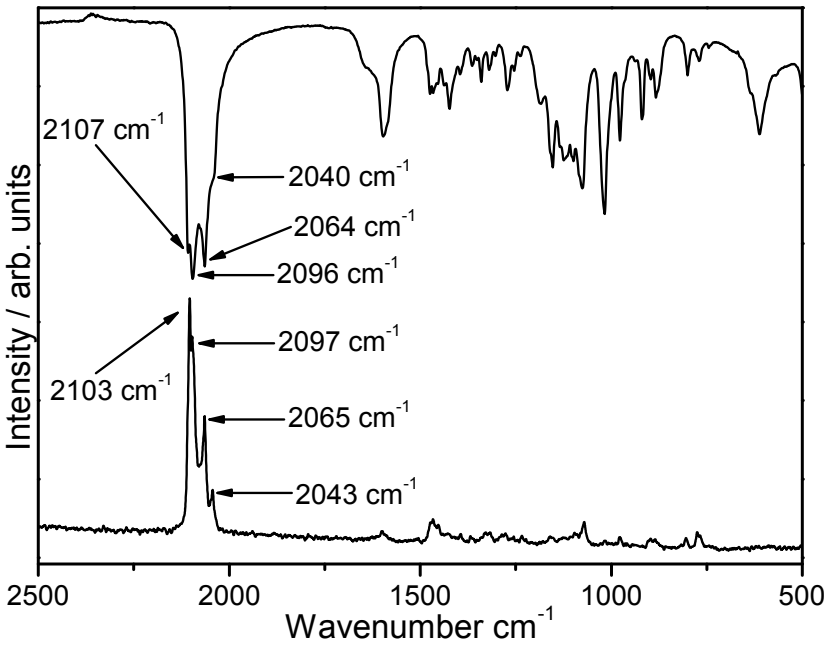

Figure S9. IR (top) and Raman (bottom) spectra for compound **3**.

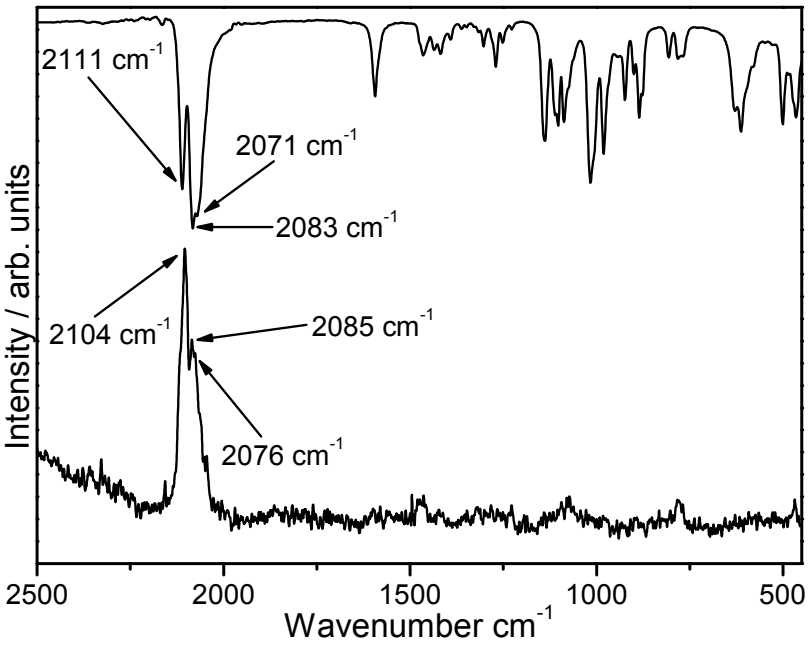

Figure S10. IR (top) and Raman (bottom) spectra for compound **4**.

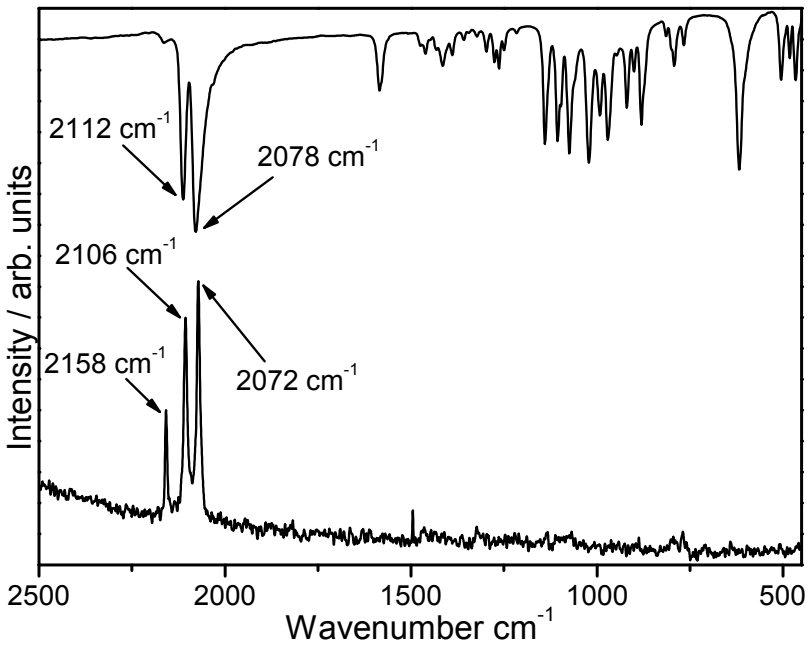

Figure S11. IR (top) and Raman (bottom) spectra for compound **5**.

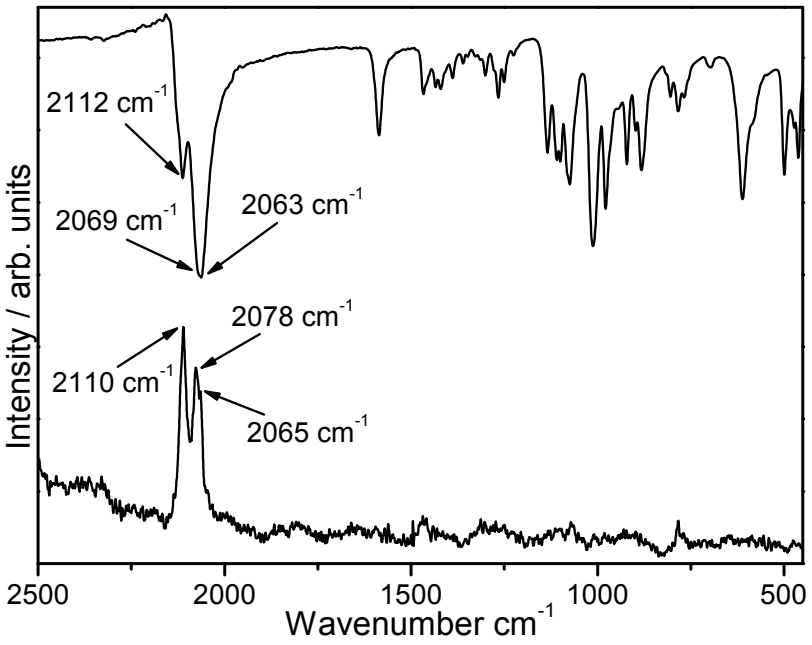

Figure S12. IR (top) and Raman (bottom) spectra of the residue obtained in thermal decomposition of compound **1I**.

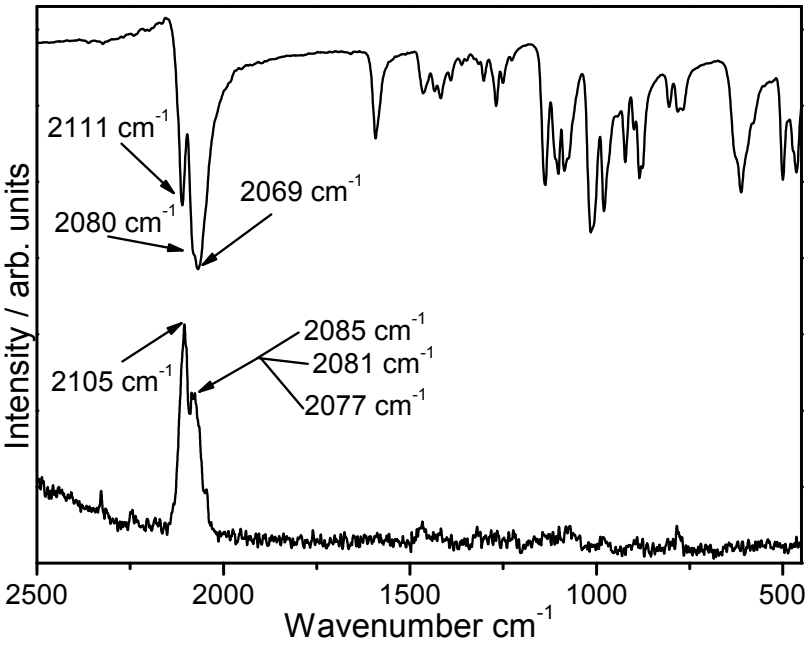

Figure S13. IR (top) and Raman (bottom) spectra of the residue obtained in thermal decomposition of compound **4**.

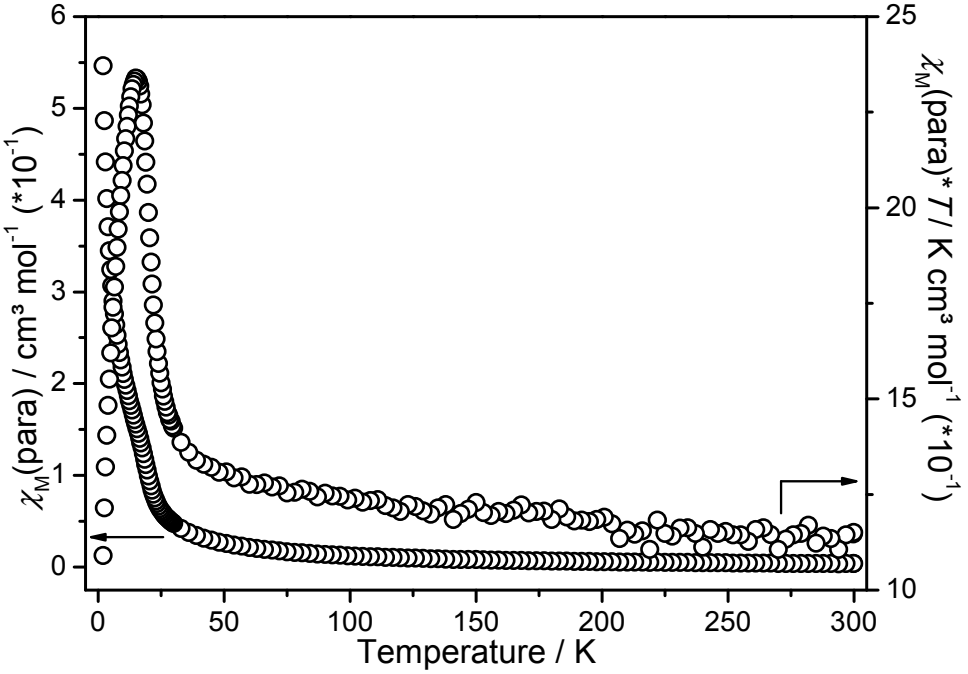

Figure S14. Results of the magnetic measurements by plots of paramagnetic susceptibility and $\chi_M T$ as function of temperature for compound **1II**.

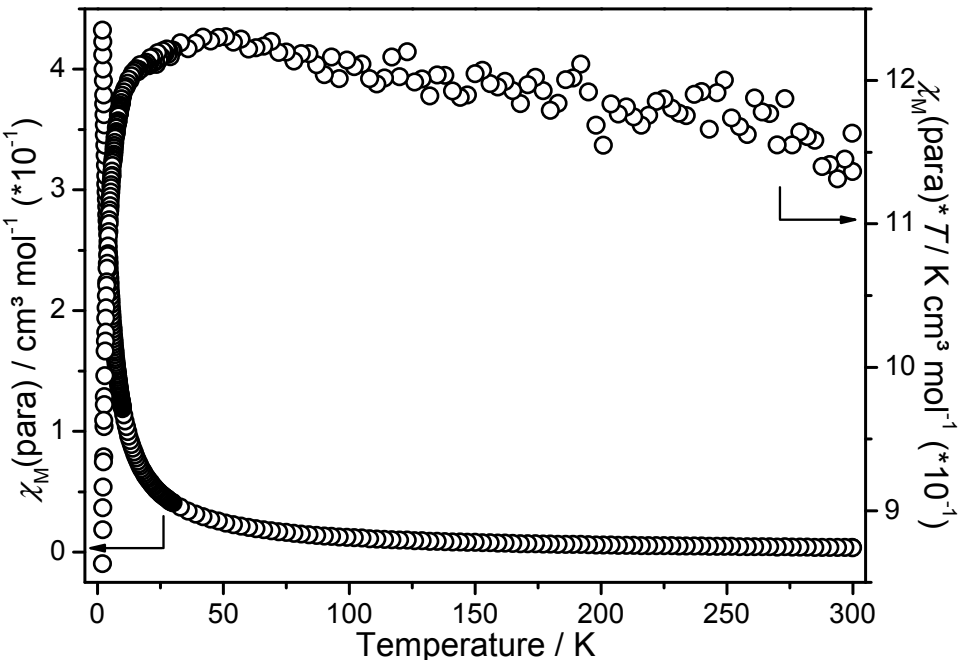

Figure S15. Results of the magnetic measurements by plots of paramagnetic susceptibility and $\chi_M T$ as function of temperature for compound **2**.

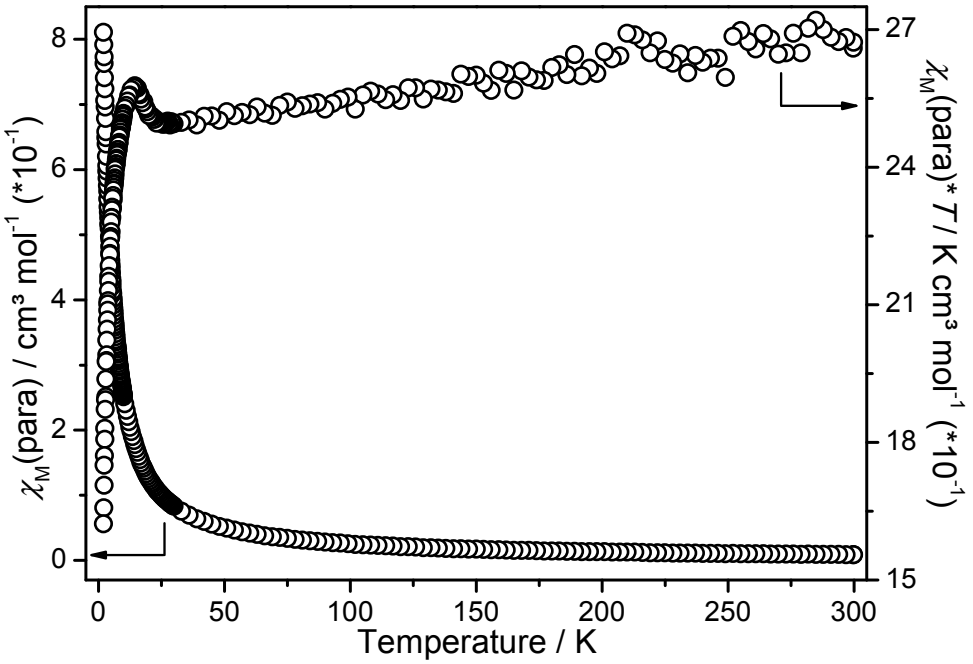

Figure S16. Results of the magnetic measurements by plots of paramagnetic susceptibility and $\chi_M T$ as function of temperature for compound **3**.

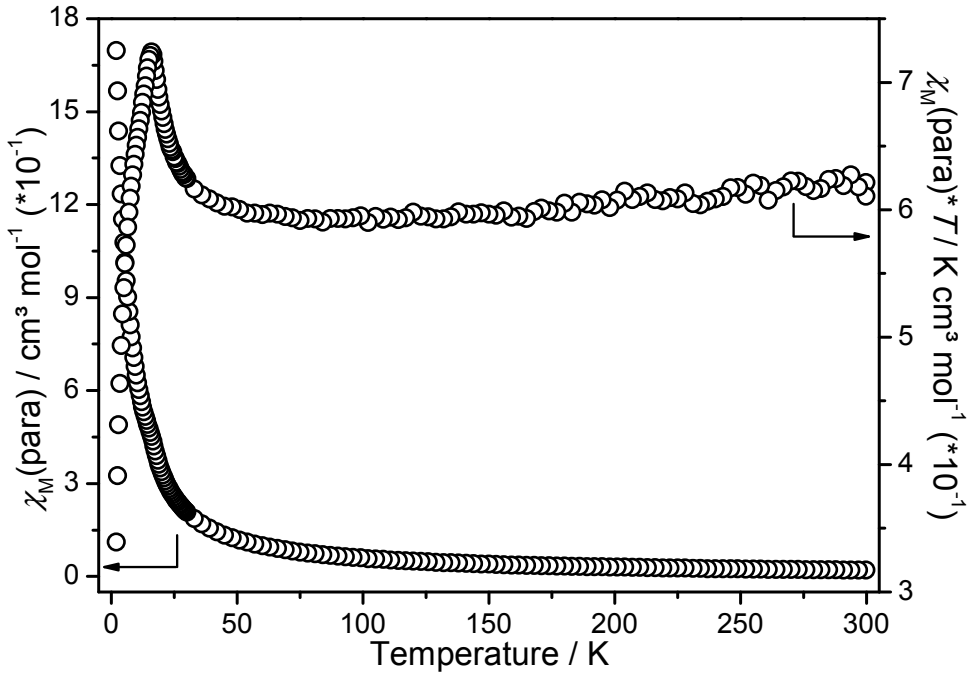

Figure S17. Results of the magnetic measurements by plots of paramagnetic susceptibility and $\chi_M T$ as function of temperature for compound **4**.

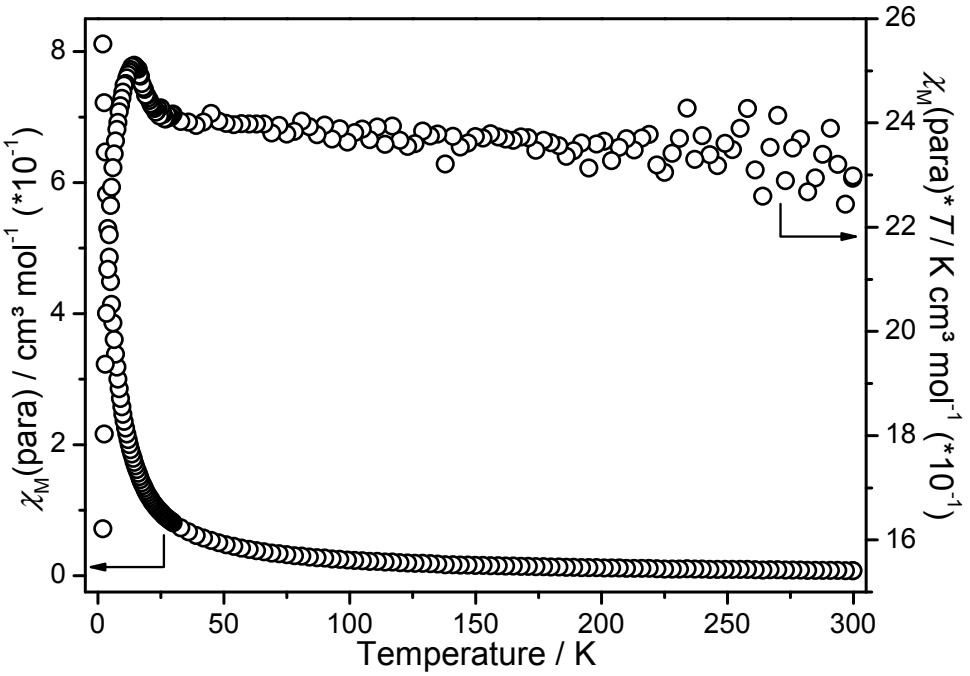

Figure S18. Results of the magnetic measurements by plots of paramagnetic susceptibility and $\chi_M T$ as function of temperature for the residue obtained after the first mass step in thermal decomposition of compound **3**.

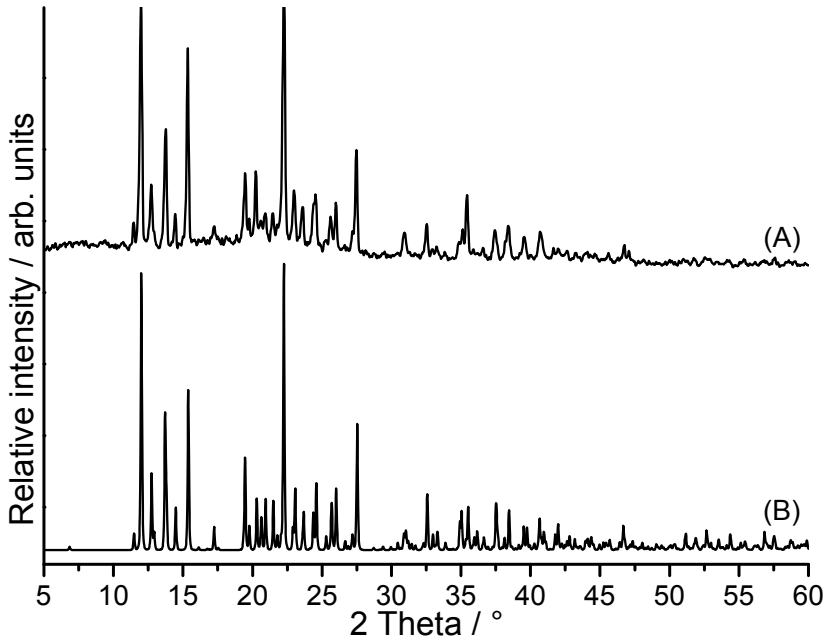

Figure S19. Experimental XRPD pattern of compound **1I** (A) together with calculated XRPD pattern from single crystal data for compound **1I** (B).

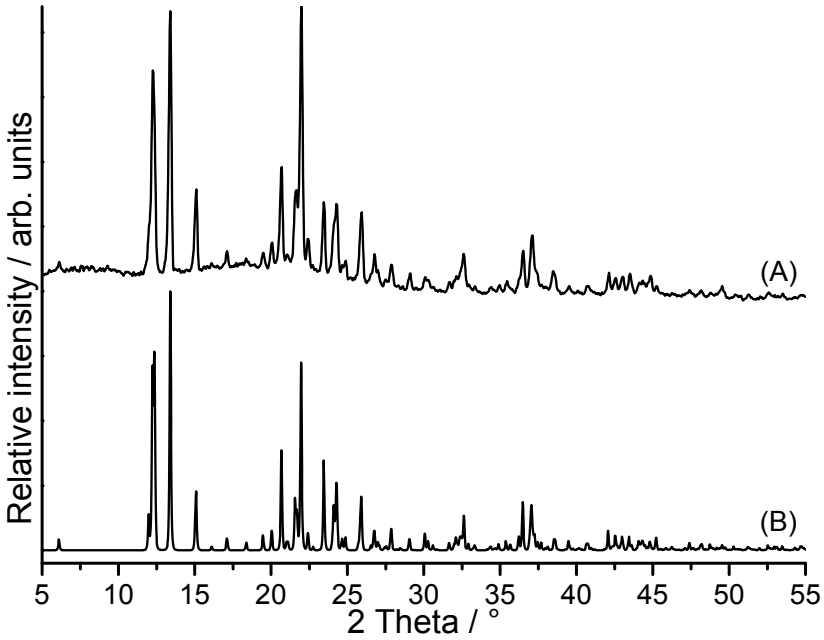

Figure S20. Experimental XRPD pattern of compound **1II** (A) together with calculated XRPD pattern from single crystal data for compound **1II** (B).

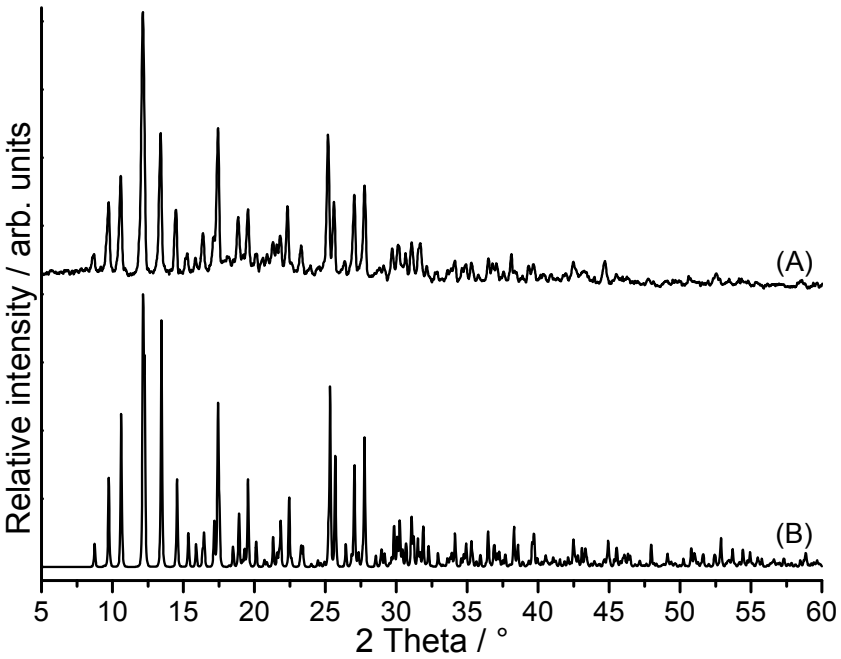

Figure S21. Experimental XRPD pattern of compound **2** (A) together with calculated XRPD pattern from single crystal data for compound **2** (B).

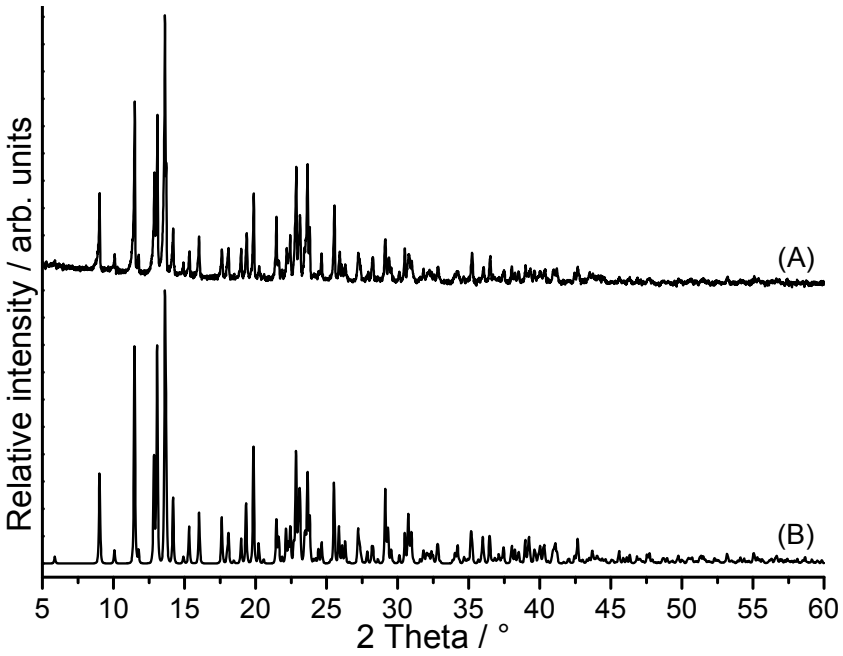

Figure S22. Experimental XRPD pattern of compound **3** (A) together with calculated XRPD pattern from single crystal data for compound **3** (B).

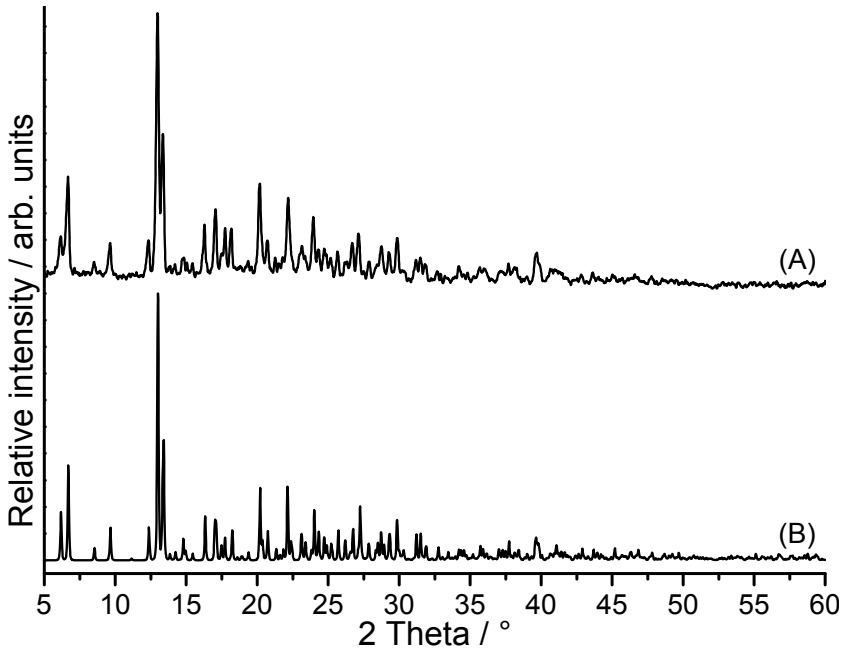

Figure S23. Experimental XRPD pattern of compound **4** (A) together with calculated XRPD pattern from single crystal data for compound **4** (B).

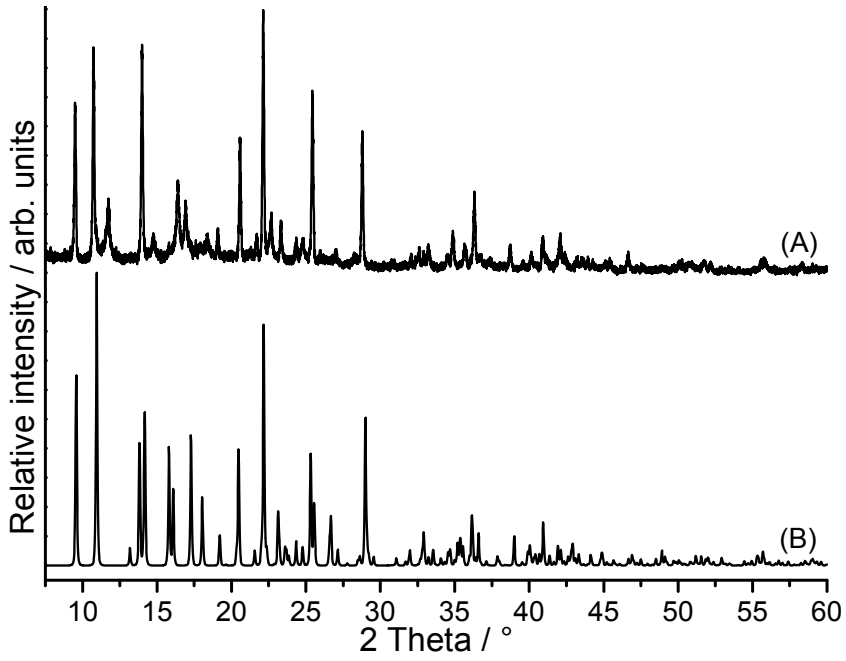

Figure S24. Experimental XRPD pattern of compound **5** (A) together with calculated XRPD pattern from single crystal data for compound **5** (B).

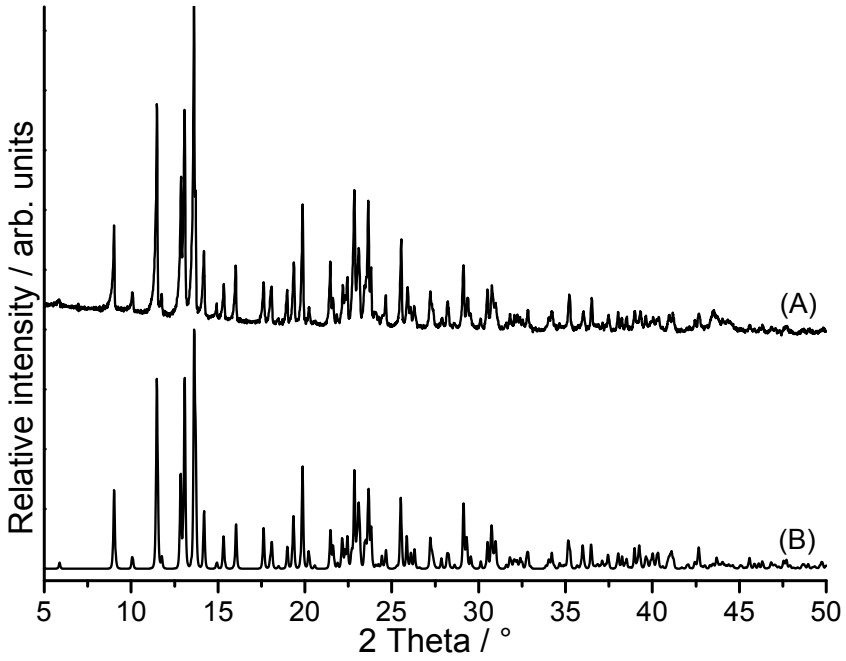

Figure S25. Experimental XRPD pattern of the residue obtained after the first mass step in thermal decomposition of compound **3** (A) together with calculated XRPD pattern from single crystal data for compound **3** (B).

Table S1. Selected bond lengths [Å] and angles [deg] for compound **1a** and **1b**.

Modification	**1a**	**1b**
Ni(1)-N(1)	2.0634(15)	2.112(2)
Ni(1)-N(2)	2.0894(15)	2.072(2)
Ni(1)-N(11)	2.1102(14)	2.092(2)
Ni(1)-N(12)	2.1478(14)	2.1386(19)
Ni(1)-N(13)	2.1108(14)	2.1093(19)
Ni(1)-N(21)	2.1660(14)	2.1879(19)
N(1)-Ni(1)-N(2)	179.69(6)	179.00(8)
N(1)-Ni(1)-N(11)	89.58(6)	90.16(8)
N(1)-Ni(1)-N(12)	90.49(6)	88.22(8)
N(1)-Ni(1)-N(13)	92.08(6)	88.05(8)
N(1)-Ni(1)-N(21)	90.85(6)	89.08(8)
N(2)-Ni(1)-N(11)	90.32(6)	90.06(8)
N(2)-Ni(1)-N(12)	89.80(6)	92.73(8)
N(2)-Ni(1)-N(13)	88.02(6)	91.65(8)
N(2)-Ni(1)-N(21)	88.86(6)	89.95(8)
N(11)-Ni(1)-N(12)	89.19(6)	95.24(8)
N(11)-Ni(1)-N(13)	178.01(6)	174.89(8)
N(11)-Ni(1)-N(21)	91.35(5)	86.74(8)
N(12)-Ni(1)-N(21)	178.56(5)	178.56(5)
N(13)-Ni(1)-N(12)	91.90(6)	91.90(6)
N(13)-Ni(1)-N(21)	87.52(5)	87.52(5)

Table S2. Selected bond lengths [Å] and angles [deg] for compound **2**.

Ni(1)-N(11)	2.179(2)	N(12)-Ni(1)-N(13)	90.34(9)
Ni(1)-N(12)	2.178(2)	N(12)-Ni(1)-N(21)	87.51(8)
Ni(1)-N(13)	2.115(2)	N(12)-Ni(1)-N(22)	178.91(8)
Ni(1)-N(21)	2.184(2)	N(12)-Ni(1)-N(23)	90.04(9)
Ni(1)-N(22)	2.202(2)	N(13)-Ni(1)-N(21)	87.75(8)
Ni(1)-N(23)	2.119(2)	N(13)-Ni(1)-N(22)	89.75(8)
N(11)-Ni(1)-N(12)	92.70(9)	N(13)-Ni(1)-N(23)	96.26(9)
N(11)-Ni(1)-N(13)	173.76(8)	N(21)-Ni(1)-N(22)	93.58(8)
N(11)-Ni(1)-N(21)	86.94(8)	N(21)-Ni(1)-N(23)	175.31(9)
N(11)-Ni(1)-N(22)	87.31(8)	N(22)-Ni(1)-N(23)	88.87(8)
N(11)-Ni(1)-N(23)	89.19(9)		

Table S3. Selected bond lengths [Å] and angles [deg] for compound **3**.

Ni(1)-N(11)	2.152(8)	Ni(2)-N(2)	2.103(10)
Ni(1)-N(12)	2.207(8)	Ni(2)-N(3)	2.140(9)
Ni(1)-N(13)	2.135(8)	Ni(2)-N(4)	2.089(9)
Ni(1)-N(21)	2.152(8)	Ni(2)-N(31)	2.092(10)
Ni(1)-N(22)	2.189(7)	Ni(2)-N(32)	2.130(8)
Ni(1)-N(23)	2.114(8)	Ni(2)-N(33)	2.070(8)
N(11)-Ni(1)-N(12)	91.1(3)	N(2)-Ni(2)-N(3)	92.0(4)
N(11)-Ni(1)-N(13)	174.3(4)	N(2)-Ni(2)-N(4)	89.6(4)
N(11)-Ni(1)-N(21)	88.4(3)	N(2)-Ni(2)-N(31)	84.4(4)
N(11)-Ni(1)-N(22)	86.4(3)	N(2)-Ni(2)-N(32)	178.5(4)
N(11)-Ni(1)-N(23)	90.5(3)	N(2)-Ni(2)-N(33)	88.1(4)
N(12)-Ni(1)-N(13)	92.0(3)	N(3)-Ni(2)-N(4)	176.9(4)
N(12)-Ni(1)-N(21)	88.8(3)	N(3)-Ni(2)-N(31)	86.6(4)
N(12)-Ni(1)-N(22)	177.1(3)	N(3)-Ni(2)-N(32)	88.5(3)
N(12)-Ni(1)-N(23)	88.7(3)	N(3)-Ni(2)-N(33)	91.4(4)
N(13)-Ni(1)-N(21)	86.9(3)	N(4)-Ni(2)-N(31)	90.9(4)
N(13)-Ni(1)-N(22)	90.5(3)	N(4)-Ni(2)-N(32)	89.8(3)
N(13)-Ni(1)-N(23)	94.3(3)	N(4)-Ni(2)-N(33)	91.3(4)

Table S4. Selected bond lengths [Å] and angles [deg] for compound **4**.

Ni(1)-S(1)	2.7142(11)	N(3)-Ni(2)-N(22)	90.72(14)
Ni(1)-N(1A)	2.098(3)	N(3)-Ni(2)-N(23)	92.08(18)
Ni(1)-N(2)	2.035(3)	N(4)-Ni(2)-O(1W)	86.0(2)
Ni(1)-N(11)	2.080(3)	N(4)-Ni(2)-O(1W')	93.5(4)
Ni(1)-N(12)	2.102(3)	N(4)-Ni(2)-N(21)	87.27(15)
Ni(1)-N(13)	2.082(3)	N(4)-Ni(2)-N(22)	91.31(13)
N(1A)-Ni(1)-S(1)	88.74(8)	N(11)-Ni(1)-S(1)	84.66(9)
N(1A)-Ni(1)-N(12)	90.36(11)	N(11)-Ni(1)-N(1A)	89.97(11)
Ni(2)-O(1W)	2.133(7)	N(11)-Ni(1)-N(12)	96.22(11)
Ni(2)-O(1W')	2.238(16)	N(11)-Ni(1)-N(13)	170.49(12)
Ni(2)-N(3)	2.060(4)	N(12)-Ni(1)-S(1)	178.74(8)
Ni(2)-N(4)	2.091(3)	N(13)-Ni(1)-N(1A)	87.11(12)
Ni(2)-N(21)	2.125(4)	N(13)-Ni(1)-S(1)	86.22(9)
Ni(2)-N(22)	2.094(3)	N(13)-Ni(1)-N(12)	92.85(12)
Ni(2)-N(23)	2.072(4)	N(21)-Ni(2)-O(1W)	79.0(2)
N(2)-Ni(1)-S(1)	87.63(9)	N(21)-Ni(2)-O(1W')	98.3(5)
N(2)-Ni(1)-N(1A)	176.33(13)	N(22)-Ni(2)-O(1W)	173.19(18)
N(2)-Ni(1)-N(11)	90.15(12)	N(22)-Ni(2)-O(1W')	166.3(4)
N(2)-Ni(1)-N(12)	93.27(12)	N(22)-Ni(2)-N(21)	94.66(15)
N(2)-Ni(1)-N(13)	92.19(12)	N(23)-Ni(2)-O(1W)	92.7(2)
N(3)-Ni(2)-O(1W)	92.0(2)	N(23)-Ni(2)-O(1W')	74.0(5)
N(3)-Ni(2)-O(1W')	84.6(4)	N(23)-Ni(2)-N(4)	88.25(14)
N(3)-Ni(2)-N(4)	177.92(15)	N(23)-Ni(2)-N(21)	170.83(16)
N(3)-Ni(2)-N(21)	92.11(19)	N(23)-Ni(2)-N(22)	93.44(15)

Table 5. Selected bond lengths [Å] and angles [deg] for compound **5**.

Ni(1)-S(2)	2.6404(19)	N(2A)-Ni(1)-S(2)	92.14(16)
Ni(1)-N(1)	2.070(5)	N(2A)-Ni(1)-N(11)	89.6(2)
Ni(1)-N(2A)	2.055(5)	N(2A)-Ni(1)-N(12)	93.6(2)
Ni(1)-N(11)	2.069(6)	N(2A)-Ni(1)-N(13)	91.5(2)
Ni(1)-N(12)	2.092(5)	N(11)-Ni(1)-S(2)	87.75(19)
Ni(1)-N(13)	2.099(6)	N(11)-Ni(1)-N(12)	91.7(3)
N(1)-Ni(1)-S(2)	87.24(16)	N(11)-Ni(1)-N(13)	172.2(2)
N(1)-Ni(1)-N(2A)	179.4(2)	N(12)-Ni(1)-S(2)	174.24(18)
N(1)-Ni(1)-N(11)	90.5(2)	N(12)-Ni(1)-N(13)	95.9(3)
N(1)-Ni(1)-N(12)	87.0(2)	N(13)-Ni(1)-S(2)	84.51(18)
N(1)-Ni(1)-N(13)	88.3(2)		

Table 6. Stretching vibration $\nu_{as}[\nu(CN)]$ band in the infrared (4000–400 cm^{-1}) and Raman spectra (3500-100 cm^{-1}) for the thiocyanato anions in compounds **1a-5** and the residues of **1a** and **4**.

Compound	IR bands [cm^{-1}]	Raman bands [cm^{-1}]
1a	2088 vs	2088 vs
1b	2077 vs	2077 vs
2	2074 m, 2050 vs, 2028 vs	2076 m, 2050 vs, 2032 vs
3	2107 vs, 2096 vs, 2064 vs, 2040 m	2103 vs, 2097 vs, 2065 m, 2043 w
4	2111 vs, 2083 vs, 2071 vs	2104 vs, 2085 vs, 2076 vs
5	2112 vs, 2078 vs	2158 m, 2106 vs, 2072 vs
residue **1a**	2112 m, 2069 vs, 2063 vs	2110 vs, 2078 vs, 2065 m
residue of **4**	2111 m, 2080 vs, 2069 vs	2105 vs, 2085 vs, 2081 vs, 2077 vs

vs = very strong; m = mid; w = weak.